ADVANCES IN FOREST FIRE RESEARCH

2022

Edited by

DOMINGOS XAVIER VIEGAS

LUÍS MÁRIO RIBEIRO

Assessing the role played by meteorological conditions on the interannual variability of fire activity in four subregions of Iberia

Sílvia A. Nunes*[1]; Carlos C. DaCamara[1]; José M. C. Pereira[2]; Ricardo M. Trigo[1]

[1]*Instituto Dom Luiz (IDL), Faculdade de Ciências, Universidade de Lisboa, 1749-016 Lisbon, Portugal, {sanunes, cdcamara, rmtrigo}@fc.ul.pt*
[2]*Centro de Estudos Florestais, Instituto Superior de Agronomia, Universidade de Lisboa, 1349-017, Lisbon, Portugal {jmcpereira@isa.ulisboa.pt}*

**Corresponding author*

Keywords

Fire activity; Fire Radiative Power; Two generalized Pareto tail lognormal body distribution; Iberian Peninsula; Fire Weather Index

Abstract

The Iberian Peninsula is recurrently affected by severe wildfires resulting from an interplay of human activities, landscape features, and atmospheric conditions. Here we assess the role played by atmospheric conditions on wildfire activity as measured by Fire Radiative Power (FRP) derived from observations by the MODIS instrument. The study spans the period 2001-2020 and is performed in four pyroregions covering the Iberian Peninsula that have been used in recent years, namely the northwest (NW), southwest (SW), north (N) and east (E). Atmospheric conditions are characterized by means of the Fire Weather Index (FWI), which rates fire intensity. For each pyrogegion, the distribution of $\log_{10} FRP$ is characterized by means of a statistical model that combines a truncated lognormal distribution central body with a lower and an upper tail, both consisting of Generalized Pareto (GP) distributions. The model is then improved by using FWI as a covariate of the parameters of the lognormal and the two GP distributions. Then, for each pyroregion, a set of 100 synthetic time series of total annual FRP is set up using the statistical models with and without FWI as a covariate. The role played by meteorological conditions is finally assessed by comparing the two sets between each other and against the time series of annual FRP derived from observations by the MODIS instrument. Results obtained for region SW show an increase from 90% to 96% of interannual explained variance of FRP when progressing from the model without to the model with FWI as covariate. Increases from 95% to 96%, 84% to 89% and from 79% to 86% were obtained for regions NW, N and E. It is worth stressing that these are conservative estimates of change, since the dependence of number of ignitions on FWI was not taken into account.

1. Introduction

The Iberian Peninsula is recurrently affected by severe wildfires that relate to an increase in fuel availability due to land abandonment and the expansion of forest and shrubland areas (Pausas and Vallejo, 1999; Lloret et al., 2002), as well as to an increase in the occurrence of prolonged droughts and in the number of days with extreme fire weather associated to climate change (Pereira et al., 2005; Trigo et al., 2006; Carvalho et al., 2011; Pereira et al., 2013; Sousa et al., 2015; Pérez-Sánchez et al., 2019; Turco et al., 2019).

The Iberian Peninsula has been affected by large wildfires in the recent decades, and the tragic years of 2003, 2005 and 2017 in Portugal are worth being pointed out. The Iberian Peninsula was struck by a severe heat wave in August 2003 and by two severe heatwaves in 2017 (the first in mid-June and the second in the second week of July), and 2005 and 2017 were affected by two severe droughts, that of 2005 being the most severe in recent times (Garcia-Herrera et al., 2007). Several studies have underlined the critical role played by different meteorological variables, including temperature, humidity and wind on the occurrence of extreme years of fire activity both at shorter (e.g. summer heat waves) and longer (e.g. prolonged droughts) time scales (Ruffault et al., 2020).

The fact that the entire Mediterranean basin, and the Iberian Peninsula in particular, is considered as a hotspot of climate change, increases the likelihood of occurrence of extreme fire weather and of more intense droughts (Turco et al., 2019; Ruffault et al., 2020). This strongly suggests that particular attention should be devoted to the role played by atmospheric conditions on wildfire activity. The aim of this work is to assess the impact of meteorological conditions on the interannual variability of fire activity in four pyroregions of the Iberian Peninsula (Trigo et al., 2016).

2. Data and Methods

The study area comprises four pyroregions in the Iberia Peninsula (Northwestern, Northern, Southwestern and Eastern) as identified by Trigo, et al. (2016) based on a cluster analysis of monthly burned area (Fig.1).

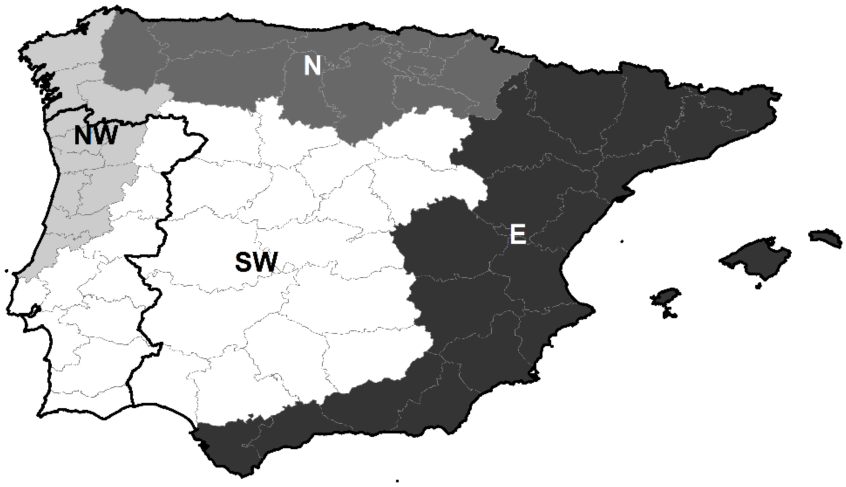

Figure 1- The four pyroregions of the Iberian Peninsula: Northwestern (NW), Northern (N), Southwestern (SW) and Eastern (E). Adapted from Trigo et al. (2016)

Fire activity is measured by the radiative power released by wildfires, as measured by the MODIS instrument on-board Terra and Aqua satellites (Giglio et al., 2020) and meteorological fire danger was rated using the Fire Weather Index (FWI), an index of fire danger that rates fire intensity (Stocks et al., 1989).

Information about Fire Radiative Power (FRP) was obtained from Collection 6 Terra and Aqua MODIS fire product covering the 20-year period from 2001 to 2020 (Giglio et al., 2020). Information about FWI covering the same period was obtained from ECMWF ERA5 reanalysis (CEMS, 2019).

For each pyroregion, a statistical model is adjusted to the distribution of the decimal logarithm of fire radiative power, $\log_{10} FRP$, and the model is then improved by incorporating FWI as a covariate of the model. The statistical models of $\log_{10} FRP$ combine three components, namely a truncated lognormal distribution central body with a lower and an upper tail, both consisting of Generalized Pareto (GP) distributions. For each pyroregion, the eight parameters of the model (namely the two points separating the central body from the tails, the location and dispersion parameters of the central truncated lognormal and the scale and shape parameters of the GP distributions of the tails) are obtained by maximizing the joint log-likelihood of an i.i.d. sample of $\log_{10} FRP$.

Finally, for each pyroregion a set of 100 synthetic time series of annual values of FRP is generated using the statistical model without FWI as covariate according to the following procedure: for each hotspot detected by the MODIS instrument, a random value of probability is generated and the corresponding value of FRP is obtained by inverting the statistical model. A time series of synthetic annual values of FRP is then obtained by adding up the generated values of FRP on a yearly basis. This process is then repeated 100 times. A second set of 100 synthetic time series of annual values of FRP is generated, this time using the model with FWI as covariate. The procedure is identical to the preceding one, with the difference lying in that FRP values are synthesized using a randomly generated probability value, together with the observed FWI value at each hotspot. The role played by meteorological conditions is finally assessed by comparing the two sets between each other and against the time series of annual FRP derived from observations by the MODIS instrument.

3. Results and discussion

Figure 2 provides an overview of results obtained when fitting, for each pyroregion, the statistical models to the samples of observed values of $\log_{10} FRP$ for the period 2001-2020. Cumulative distribution functions of the fitted model closely follow the corresponding empirical cumulative distribution function derived from the samples, and this reflects on Q-Q plots that closely follow the 1:1 straight lines. Pyroregion NW presents the higher probabilities of exceedance for values of $\log_{10} FRP$ between 0.5 and 2 whereas the lower values of exceedance are found in pyroregion E for values of $\log_{10} FRP$ between 0.5 and 1.5 and in pyroregion N for values of $\log_{10} FRP$ between 1.5 and 2.

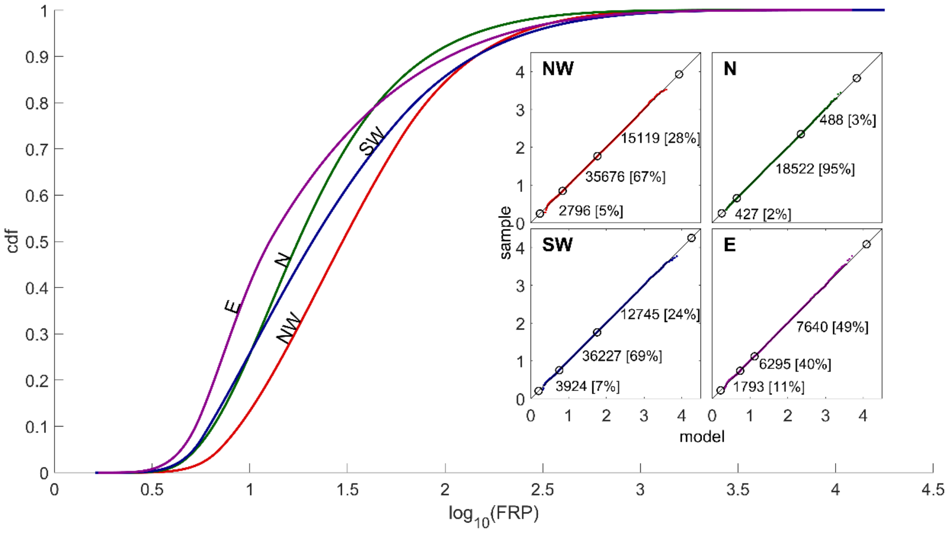

Figure 2 – Cdf curves and Q-Q plots (inside squares) of fitted statistical models of log_10 FRP (in MW) for regions NW (red), N (green) SW (blue), and E (magenta). The open circles in the 1:1 lines of the QQ plots delimit the central body and the upper and lower tails of the distributions, and the small colored dots represent the fire events of the sample. For each pyroregion, the number of events and respective fraction (in brackets) of the sample in the central body and in the lower and upper tails of the distribution are indicated next to the 1:1 line of the respective Q-Q plot

Figure 3 illustrates the results obtained when FWI is added as a covariate of the parameters of the distributions. As might be expected, there is a right displacement of the cumulative distribution functions with increasing FWI, which reflects substantial increases in probability of exceedance of a given threshold of $\log_{10} FRP$.

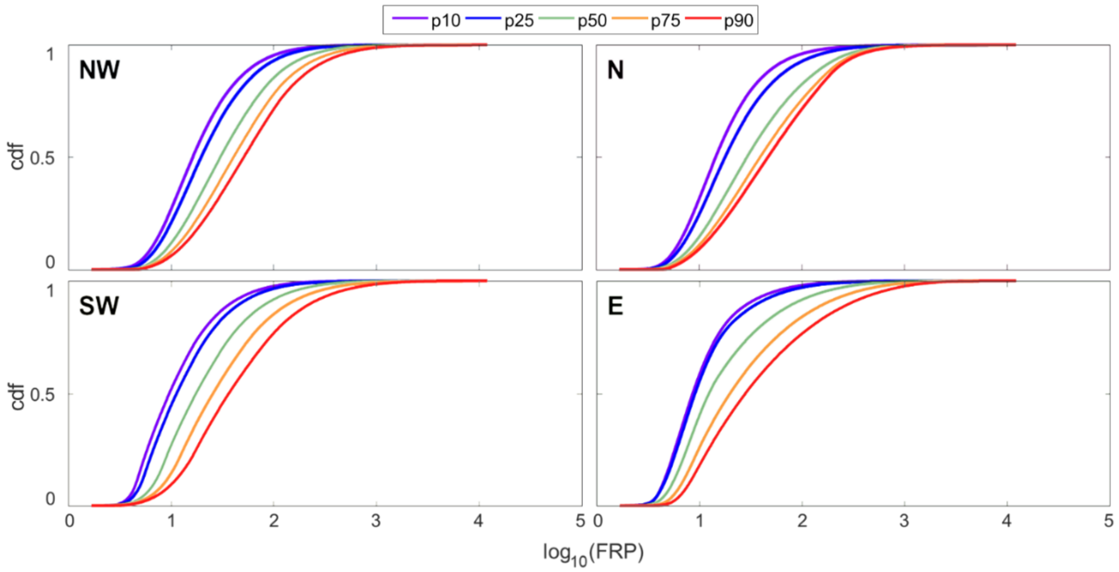

Figure 3 –Sensitivity to FWI of cumulative distribution functions of fitted statistical models of $log_{10}FRP$ (in MW) for the four subregions. Colors of each curve identify the prescribed value of FWI, respectively percentiles 10 (purple), 25 (blue), 50 (green), 75 (orange) and 90 (red) of the respective samples.

Figure 4 presents, for each ecoregion, the time series of annual FRP as derived from observations by the MODIS instrument (black curves) and the two time series obtained by averaging the two sets of 100 annual values of FRP as derived from the statistical models without (green curve) and with (red curve) FWI as covariate. The interannual variability of the time series generated by the model without FWI as covariate is just due to the interannual variability of hotspots observed by the MODIS instrument, and it is worth noting that some years with large (small) values of total FRP tend to be underestimated (overestimated). The underestimation is conspicuous in 2017 for pyroregions NW and N, in 2003 for pyroregion SW, and in 2012 for pyregion E, whereas the overestimation, although less pronounced, occurs e.g. in 2014 for pyroregion N and in 2007 and 2008 for pyroregion SW. In the case of the time series generated by the model with FWI, an improved behavior is observed that is particularly noticeable for years with large values of total FRP, where synthetic values obtained from the model with FWI are much closer to observed values than synthetic values from the model where meteorological conditions are disregarded.

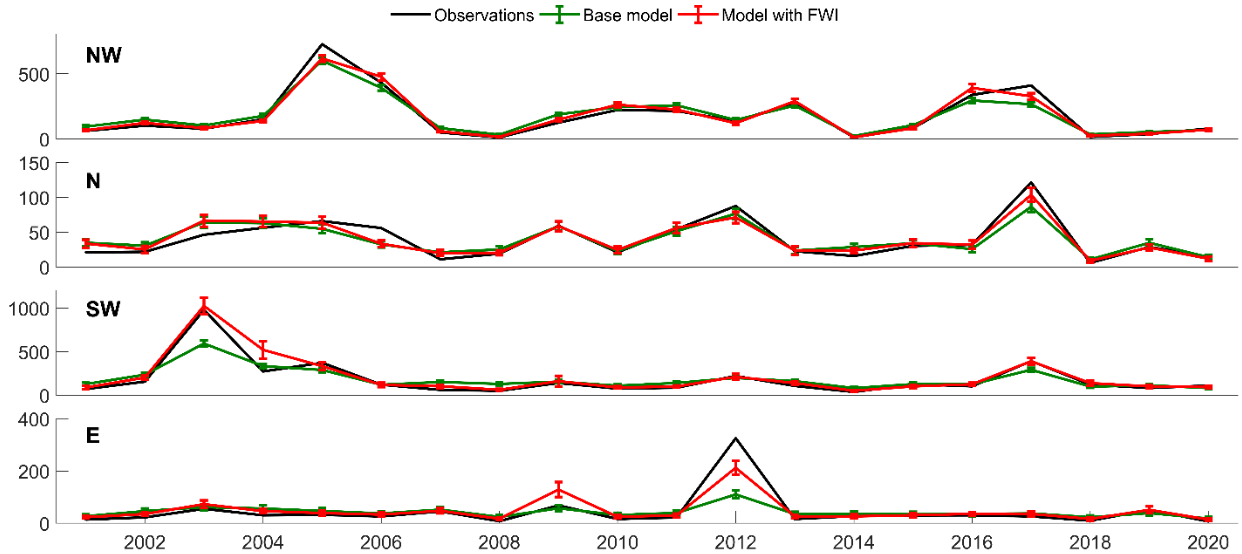

Figure 4 – Time series, for each pyroregion, of annual values of observed (black curves) and of the mean values of the set of synthetically generated annual values of FRP using the statistical models without (green curves) and with (red curves) FWI as covariate. The error bars in the synthetic time series delimit the mean plus/minus one standard deviation.

A quantitative assessment is provided in Table 1, which presents the mean and the standard deviation of the time series of annual FRP derived from MODIS observations and of the annual FRP synthetically generated by the statistical models without and with FWI as covariate. Results indicate that synthetic time series generated by both models are unbiased, the only exception being pyroregion E, where the time series generated by the model with FWI as covariate presents a mean value 12% larger than the mean of time series of observed FRP. Considerable differences do, however, occur with the values of standard deviation, for which time series of synthetically generated FRP present considerably lower values than the corresponding time series of observed FRP. However, time series generated using the model with FWI as covariate systematically display larger variability than the corresponding ones obtained with the model lacking FWI as covariate. For instance, there is an 11% increase (from 21 to 24 GW) for pyroregion N, a 17% increase (from 143 to 167 GW) for pyroregion NW, a 48% increase (from 121 to 179 GW) for pyroregion SW and a 230% increase (from 20 to 46 GW) for pyroregion E. These results indicate that atmospheric conditions are especially important to better reproduce interannual variability in the case of pyroregions E and SW.

Table 1 also presents, for each pyroregion, the explained variance accounted for the synthetic series when they are used to simulate interannual variability. Explained variance was estimated by squaring the linear correlation of the time series of annual observed FRP with the corresponding synthetic time series generated by the statistical models lacking and including FWI as covariate. For all pyroregions there is an increase in explained variance when shifting from synthetic values of annual FRP generated by the models without FWI as covariate to those by the models with FWI. Increases in explained variance are modest for pyroregion NW (95 to 96%), and are even larger for the other three pyroregions N, SW and E (84 to 89%, 90 to 96% and 79 to 86%, respectively).

Table 1 – Mean value and standard deviation for the period 2001-2020 of time series of annual FRP derived from observations by the MODIS instrument and from the mean of the 100 synthetically generated annual FRP using the statistical models without and with FWI as covariate, and explained variance as obtained by squaring the linear correlation between the observed and each the two synthetic time series of annual FRP.

		NW	N	SW	E
Mean [GW]	Observed	179	40	185	43
	Model without FWI	180	40	184	42
	Model with FWI	179	40	186	47
Standard Deviation [GW]	Observed	181	29	211	68
	Model without FWI	143	21	121	20
	Model with FWI	167	24	179	46
Variance Explained [%]	Model without FWI	95	84	90	79
	Model with FWI	96	89	96	86

4. Conclusion

Results obtained clearly indicate the importance of atmospheric conditions as drivers of interannual variability in fire activity, measured by annual FRP values. This is especially true in pyroregions SW and E, where climate change is expected to have a pronounced impact in terms of increase in frequency both of drought events and of days with extreme fire weather (Sousa et al., 2015).

It is worth pointing out that the assessment performed in this work is likely to be conservative, given that time series of annual FRP were estimated by randomly generating values for all hotspots identified by the MODIS instrument for the study period. Since the number of hotspots strongly depends on the number of large fire events, which in turn depend on atmospheric conditions, the interannual variability of synthetically generated time series of FRP was very likely overestimated when using the model without FWI as covariate. Circumventing this problem would imply modelling the interannual variability of hotspots (with and without FWI as covariate), a task that is well beyond the purpose of the present work.

Models such as the ones proposed in this study provide valuable information about fire activity in the Iberian Peninsula, namely when comparing different scenarios of climate change. On the other hand, following a methodology previously developed by some of the authors (DaCamara et al., 2014; Pinto et al., 2018), the proposed models with FWI can be used to calibrate FWI in four pyroregions of the Iberian Peninsula and then define classes of fire danger that represent an important added value in fire prevention and firefighting of rural and forest fires.

5. Acknowledgments

This work was supported by national funds through FCT (Fundação para a Ciência e a Tecnologia, Portugal) under project FIRECAST (PCIF/GRF/0204/2017), IDL (UIDB/50019/2020) and CEF (UIDB/00239/2020) and by EUMETSAT Satellite Application Facility on Land Surface Analysis (LSA SAF).

6. References

Carvalho AC, Carvalho A, Martins H, Marques C, Rocha A, Borrego C, Viegas DX, Miranda AI. 2011. Fire weather risk assessment under climate change using a dynamical downscaling approach. *Environ. Model. Softw.* **26** (9), 1123–1133. https://doi.org/10.1016/j.envsoft.2011.03.012 Elsevier Ltd.

CEMS. Fire danger indices historical data from the Copernicus Emergency Management Service. 2019. ECMWF https://doi.org/10.24381/cds.0e89c522.

DaCamara CC, Calado TJ, Ermida SL, Trigo IF, Amraoui M, Turkman KF. 2014. Calibration of the Fire Weather Index over Mediterranean Europe based on fire activity retrieved from MSG satellite imagery. *International Journal of Wildland Fire* **23**, 945-958. https://dx.doi.org/10.1071/WF13157.

García-Herrera R, Paredes D, Trigo RM, Trigo IF, Hernández H, Barriopedro D, Mendes MT. 2007. The outstanding 2004–2005 drought in the IberianPeninsula: associated atmospheric circulation. *J. Hydrometeorol.* **8**, 483–498. https://dx.doi.org/10.1175/JHM578.1.

Giglio L, Schroeder W, Hall JV, Justice CO. 2020. MODIS Collection 6 Active Fire Product User's Guide. https://modis-fire.umd.edu/files/MODIS_C6_Fire_User_Guide_C.pdf (Last accessed 29 March 2022).

Lloret F, Calvo E, Pons X, Díaz-Delgado R. 2002. Wildfires and landscape patterns in the Eastern Iberian Peninsula. *Landsc. Ecol*. **17**: 745 – 759. https://doi.org/10.1023/A:1022966930861

Pausas JG, Vallejo R. 1999. The role of fire in European Mediterranean ecosystems. *Remote Sensing of Large Wildfires in the European Mediterranean Basin*, Chuvieco E (ed). Springer-Verlag: Berlin; 3 – 16. https://doi.org/10.1007/978-3-642-60164-4_2

Pereira MG, Trigo RM, DaCamara CC, Pereira JMC, Solange ML. 2005. Synoptic patterns associated with large summer forest fires in Portugal. *Agric. For. Meteorol.* **129**: 11 – 25, https://doi.org/10.1016/j.agrformet.2004.12.007.

Pereira M, Calado TJ, DaCamara CC, Calheiros T. 2013. Effects of regional climate change on rural fires in Portugal. *Clim. Res*. **57** (3), 187–200. https://doi.org/10.3354/cr01176.

Pérez-Sánchez J, Jimeno-Sáez P, Senent-Aparicio J, Díaz-Palmero JM, Cabezas-Cerezo JD. 2019. Evolution of burned area in forest fires under climate change conditions in southern Spain using ANN. *Applied Sciences (Switzerland)* **9** (19). https://doi.org/10.3390/app9194155.

Pinto MM, DaCamara CC, Trigo IF, Trigo RM, Turkman KF. 2018. Fire danger rating over Mediterranean Europe based on fire radiative power derived from Meteosat. *Natural Hazards and Earth System Sciences* **18**, 515-529. doi:10.5194/nhess-18-515-2018.

Ruffault J., Curt T., Moron V., Trigo R.M., Mouillot F., Koutsias N., Pimont F., Martin-StPaul N., Barbero R., Dupuy J.-L., Russo A., Belhadj-Khedher C., (2020) "Increased likelihood of heat-induced large wildfires in the Mediterranean Basin". Scientific Reports, 10, 13790, doi: 10.1038/s41598-020-70069-z

Sousa PM, Trigo RM, Pereira MG, Bedia J, Gutiérrez JM. 2015. Different approaches to model future burnt area in the Iberian Peninsula. *Agric. For. Meteorol*. **202**, 11–25. https://doi.org/10.1016/j.agrformet.2014.11.018.

Stocks BJ, Lawson BD, Alexander ME, Van Wagner CE, McAlpine RS, Lynham TJ, Dubé DE. 1989. The Canadian Forest Fire Danger Rating System: an overview [reprinted from August 1989 issue, 65:258-265, with corrections and new pagination]. *Forestry Chronicle* **65**(6): 450-457.

Trigo RM, Pereira JMC, Pereira MG, Mota B, Calado MT, DaCamara CC, Santo FE. 2006. Atmospheric conditions associated with the exceptional fire season of 2003 in Portugal. *Int. J. Climatol.* **26**(13):1741 – 1757. https://doi.org/10.1002/joc.1333

Trigo RM, Sousa M, Pereira MG, Rasilla D, Gouveia CM. 2016. Modelling wildfire activity in Iberia with different atmospheric circulation weather types. *Int. J. Climatol*. **36**. https://doi.org/10.1002/joc.3749

Turco M, Jerez S, Augusto S, Tarín-Carrasco P, Ratola N, Jiménez-Guerrero P, Trigo RM. 2019. Climate drivers of the 2017 devastating fires in Portugal. *Scientific Reports* **9**, 13886. doi:10.1038/s41598-019-50281-2.